Articles

Validation of the Flat Model Catalyst Approach to Olefin Polymerization Catalysis: From Catalyst Heterogenization to Polymer Morphology

Peter C. Thüne,*,† Joachim Loos,† Ulrich Weingarten,‡ Fabian Müller,‡ Winfried Kretschmer,§ Walter Kaminsky,‡ Piet J. Lemstra,† and Hans (J. W.) Niemantsverdriet†

Dutch Polymer Institute, Eindhoven University of Technology, P.O. Box 513, 5600MB Eindhoven, The Netherlands, Universität Hamburg, Bundesstrasse 45, 20146 Hamburg, Germany, and Rijksuniversiteit Groningen, Nijenborgh 4, 9747 AG Groningen, The Netherlands

Received June 26, 2002; Revised Manuscript Received November 13, 2002

ABSTRACT: Three olefin polymerization catalysts are supported onto a flat silica wafer employing spin-coating impregnation. These model catalysts feature a defined surface direction of the silica support and thus facilitate the direct correlation between catalyst dispersion and morphology of the polymer product. Depending on the interaction of the catalysts with the silica surface, the catalysts disperse in very different fashions, which induces different constraints on the polymer growth upon gas-phase polymerization. Chemical anchoring of the active species as in the CrO_x/SiO_2 (Phillips) system results in homogeneous polymer film of up to several 10 μm . In contrast the physisorbed Cp[1,3-(2,6-$Me_2C_6H_3)_2C_2H_4N_2C$═N]-$TiBz_2B(C_6F_5)_3$ forms clusters on the flat silica that evolve into highly porous, ball-shaped polymer beads. *rac*-[Me_2Si(2-Me-4-(1-Naph)Ind)$_2$]$ZrCl_2(CH_3AlO)_x$ forms a film of metallocene catalyst dispersed inside the cocatalyst matrix. Homogeneous regions of this film give rather homogeneous polymer films while local concentrations of active species (hotspots) form crater- and ball-shaped structures.

Introduction

Homogeneous olefin polymerization catalysts based on metallocene-type organometallic complexes have developed into a versatile tool to produce polymers with defined chain architecture and narrow molecular weight distribution.[1−3] The reactivity, chemo-, regio-, and stereoselectivties of these single-site catalysts can be controlled in great detail by varying the ancillary ligand or the metal center, enabling to custom make an almost unlimited range of homo- and copolymers.[4,5] However, to use this class of polymerization catalysts in existing slurry- and gas-phase reactors they have to be supported on a heterogeneous carrier. The main driving force behind these efforts to hydrogenize single site catalysts is controlling the polymer morphology to ensure a stable reactor operation and to prevent uncontrolled precipitation of polymer on the reactor walls (reactor fouling).[6] The particle replication process has been extensively studied for heterogeneous Ziegler−Natta or Cr/silica systems.[7−9]

Silica seems the natural support of choice as it allows great control of the stability of the pore structure. As the spherical catalyst particle breaks up during polymerization, the growing polymer bead remains an exact replica of the original shape. A successful heterogenization should fulfill the following criteria:

- The supported catalyst should retain its original catalytic properties.
- The active species must be evenly dispersed in the catalyst and the growing polymer bead to allow a uniform growth of the polymer particle and to prevent local overheating.
- In the case of slurry phase polymerization the catalyst must be strongly bound to the support to prevent the active site dissolving in the diluent.

Public research in the field of catalyst heterogenization has been mainly focused on the polymerization properties of the supported single site catalyst and, to a much lesser extent, the overall particle morphology.[10] An interesting approach to gain molecular level insight into different heterogenization strategies has been introduced by Duchateau et al.[11,12] who used silsesquioxanes as a homogeneous model for different groups of surface silanols.

In this paper, we want to introduce our approach to look at the heterogenization of single site catalysts is based on flat silicon wafers (silicon (100) single crystals covered with a thin layer of amorphous silica). Using basically the same preparative tools as applied for their high surface area counterparts, they have been devel-

* Corresponding author: HEW 3.50, Technische Universiteit Eindhoven. E-mail: p.c.thune@tue.nl. Telephone: 0031-(0)40 2473081. Fax: 0031- (0)40 2473481.
† Eindhoven University of Technology.
‡ Universität Hamburg.
§ Rijksuniversiteit Groningen

10.1021/ma021007z CCC: $25.00
Published on Web 02/11/2003

Scheme 1. (I) *rac*-[Me_2Si(2-Me-4-(1-Naph)Ind)$_2$]$ZrCl_2$; (II) (Cp[1,3-(2,6-$Me_2C_6H_3$)$_2C_2H_4N_2C$=N]$TiBz_2$

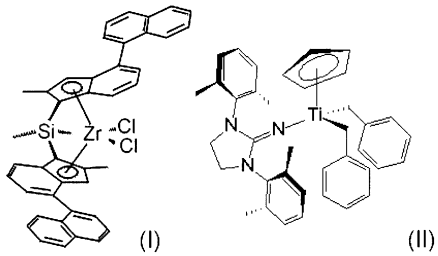

(I) (II)

oped into versatile model supports for a range of industrial important catalytic systems.[13,14] These model catalysts feature the active phase exposed on a flat (surface roughness below 1 nm) oxidic surface mounted on a conducting structural support, enabling electron and ion emitting surface spectroscopies and microscopies to be used at their full potential. The first olefin polymerization catalyst prepared on flat silica was the Cr/SiO_2 (Phillips) system, which has been described in detail in previous publications.[15−17] Within the scope of this paper we impregnate two organometallic polymerization catalysts (Scheme 1), an *ansa*-metallocene dichloride **(I)** activated with methylaluminumoxane (MAO) and a borane- ($B(C_6F_5)_3$-) activated (iminoimidazolidinato)titanium dibenzyl **(II)**. The CrO_x/SiO_2 system serves as a reference as we now examine the opportunities for the flat model catalyst approach to get a better insight in the interplay between heterogenization procedure, dispersion and morphology of the active phase and morphology of the growing polymer.

Experimental Section

Carbon monoxide (Hoekloos, 5.0), ethene (Hoekloos, 3.5), and propene (AGA polymer grade) were passed over BASF R3-11 supported Cu oxygen scavenger and molecular sieves (Aldrich, 4 Å). All experiments with the organometallic catalysts were performed under a nitrogen atmosphere using standard Schlenk or glovebox techniques. Toluene (Aldrich, anhydrous, 99.8%) was passed over columns of Al_2O_3 (Fluka), BASF R3−11 supported Cu oxygen scavenger, and molecular sieves (Aldrich, 4 Å) and degassed before use.

Spin-Coating Impregnation. The olefin polymerization catalysts are dispersed onto the flat silica wafer by spin-coating impregnation.[18] The substrate is made of a silicon (100) single-crystal disk (Topsil), which is calcined at 750 °C to produce a 90 nm thick overlayer of amorphous silica. Hydroxyl groups are introduced on the silica surface by etching with a 1/1 vol/vol mixture of ammonia solution (35%, p.a. Merck) and hydrogen peroxide (25% p.a. Merck) at 70 °C for 5 min and subsequent washing in boiling water (Millipore). After this treatment the silica surface is fully hydrozylized and features about 4−5 surface silanol groups per square nanometer.[15] The spin-coating procedure is described in detail for the Cr/silica system. Briefly the wafer is placed on a spin-coating apparatus (Laurell), covered with the impregnation solution and then rotated at several thousand rotations per minute. While most of the impregnation solution is ejected from the disk, a thin homogeneous layer stays behind. As the solvent evaporates from this layer, the solute (catalyst precursor) precipitates. The catalyst loading (m) depends on the concentration of the metal in the spin-coating solution (C_0) the density (ρ) and viscosity (η) of the solvent, the rotation speed (ϖ), and the evaporation time (t_{evap}). It can be estimated using the "loading equation" derived in[17]

$$m = 1.35 C_0 \sqrt{\frac{\eta}{\rho \varpi^2 t_{evap}}} \qquad (1)$$

$CrO_x/SiO_2/Si$(100). Chromium is impregnated as chromic acid (CrO_3) from aqueous solution (2 mmol/L) at 2800 rpm yielding a catalyst loading of 2 Cr/nm^2. The impregnated catalyst is activated in CO at 350 °C following calcination in dry O_2/Ar (20/80) at 550 °C.

***rac*-[Me_2Si(2-Me-4-(1-Naph)Ind)$_2$]$ZrCl_2$—MAO/SiO_2/Si-(100).** Silica wafers are predried at 250 °C to remove adsorbed water. The catalyst precursor **I**[19] is dissolved in toluene and activated with 15 equiv of methylaluminoxane (MAO) in toluene. The impregnation solution has a zirconium loading of 5 mmol/L and is spin-coated at 2000 rpm.

Cp[1,3-(2,6-$Me_2C_6H_3$)$_2C_2H_4N_2C$=N]$TiBz_2B(C_6F_5)_3/SiO_2$/Si(100). Silica wafers are precalcined at 750 °C to remove the majority of surface silanol groups. The pre-catalyst **II**[20] is dissolved in toluene and activated with 1.1 equiv of borane. The impregnation solution has a titanium concentration of 2.5 mmol/L and is spin-coated at 2000 rpm. The compounds Cp-[1,3-(2,6-$Me_2C_6H_3$)$_2C_2H_4N_2C$=N]$TiBz_2$ and $B(C_6F_5)_3$ were prepared according to published procedures.[21,22]

Polymerization Reactions. Polymerizations were carried out at 60−90 °C and slightly elevated pressure (1.6 bar) in a self-made quartz tube reactor.[23] Inside that reactor immediately upstream as seen from the model catalyst the ethylene was cleaned from last traces of impurities by flowing over a bed of CO-reduced chromium supported on γ-aluminum extrudates.

Microscopy. Morphological investigation of the as prepared polymer films was performed using a Philips environmental scanning electron microscope XL30 ESEM-FEG, which is equipped with a field emission electron source, using low voltage mode and a secondary electron detector. All SEM images shown here were recorded without additional sample pretreatment (e.g., surface etching, conductive coating, etc.).

Results and Discussion

All model catalysts in this preliminary series are active for ethylene polymerization and sustain their activity for several hours. Polyethylene and polypropylene formation has been affirmed by Raman and Infrared spectroscopy. However the three catalysts differ greatly in the way the active species has been dispersed onto the silica support.

A is a Philips type olefin polymerization catalyst prepared by spin-coating impregnation of aqueous chromic acid solution onto a flat silica support (silica wafer) with subsequent thermal activation in dry oxygen and reduction with carbon monoxide. This catalyst features isolated chromium atoms, which are anchored to the silica support by a direct chemical bond (surface chromates).

B is an *ansa*-zirconocene dichloride **I**, which is activated by 15 equiv of methyl aluminoxane (MAO) and impregnated onto the flat silica support. The cationic active species is supposed to be held at the support surface by weak ionic interactions with the counterion, which evolves from the MAO activator. MAO anchors to the silica surface by a condensation between the methyl aluminum functions with the surface silanol groups of the silica wafer.

C is a cyclopentadienyl(iminoimidazolidinato)titanium dibenzyl **(II)** activated with 1.1 equiv of borane ($B(C_6F_5)_3$) impregnated on precalcined (750 °C) silica wafers. The active species in this catalyst is only held on the support be weak physisorption. Surface silanol groups are depleted by calcination of the silica wafer prior to the impregnation.

In this series the strength of the catalyst support interaction decreases from catalyst **A** to catalyst **C**, which has dramatic consequences for the morphology

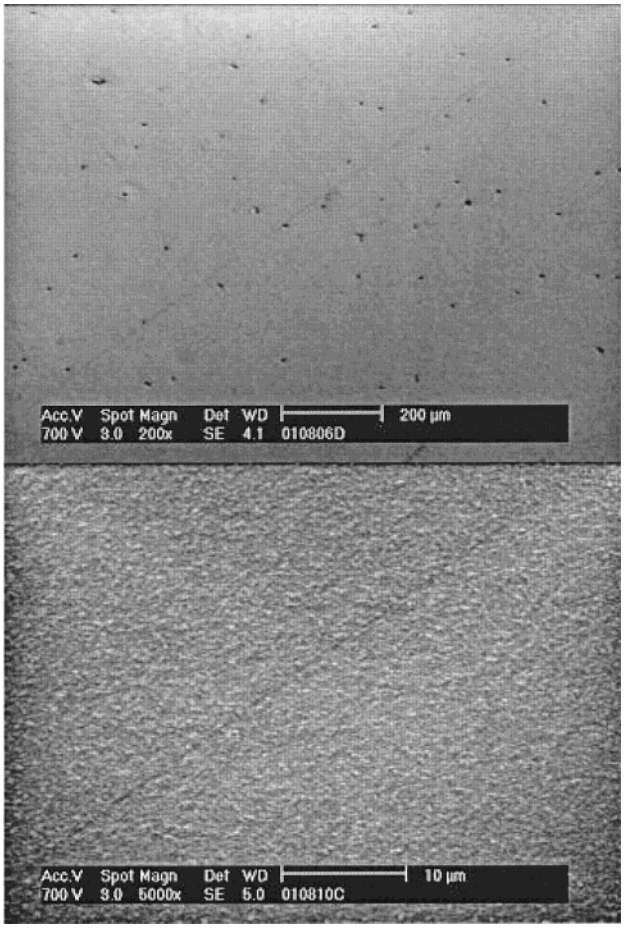

Figure 1. Surface overview (ESEM) of polyethylene film produced by $CrO_x/SiO_2/Si(100)$. Ethylene polymerization was performed at 90 °C at 1.6 bar for 12 h.

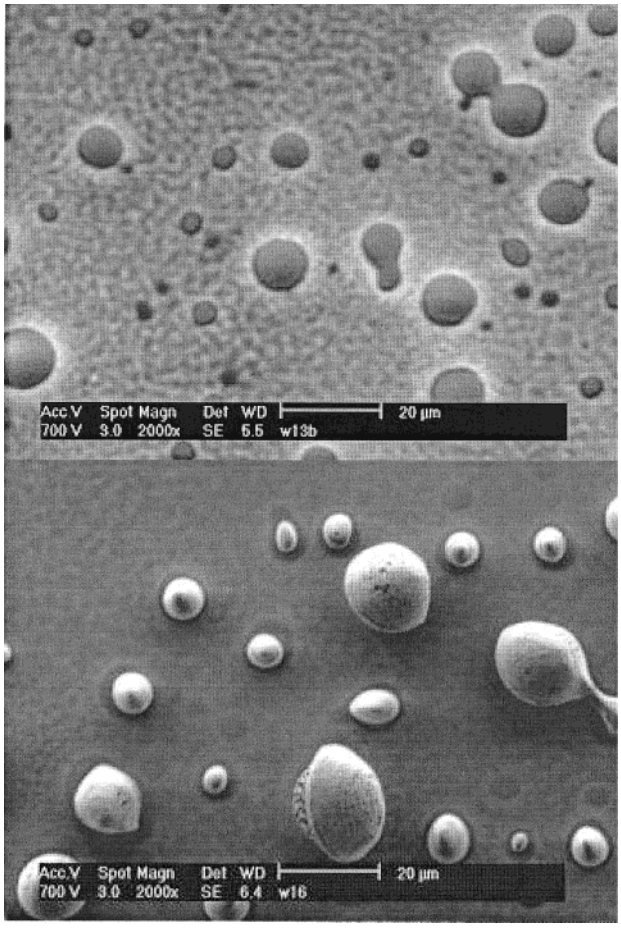

Figure 2. Surface overview of Cp[1,3-(2,6-$Me_2C_6H_3)_2C_2H_4N_2C$=N]$TiBz_2-B(C_6F_5)_3/SiO_2/Si(100)$ after spin-coating impregnation (top) and after ethylene polymerization (60 °C, 1,6 bar ethylene, 12 h, bottom).

of the polymer that evolves on these catalysts. We used scanning electron microscopy to visualize the polymer as it has grown on the flat silica support. Figure 1 shows a 20 μm thick polyethylene film produced by the $CrO_x/SiO_2/Si(100)$ system (catalyst **A**) at 90 °C (12 h polymerization at 1.6 bar C_2H_4). On the Phillips catalyst, the active sites are dispersed homogeneously on the flat silica surface and remain anchored to the support during the polymerization reaction. As the rate of polymerization remains constant on the wafer, the polymer film can only grow in the direction of the surface normal. This results in a relatively smooth homogeneous polymer film both in the millimeter and the micrometer scale. While some pinholes and stress fibrils can be observed, this film also shows a relatively high density. Occasionally some circular craters are observed in the polymer film, which presumably are induced by tiny, wet dust particles carrying catalyst poison. These craters allow a side view at the polymer layers indicating 1-dimensional pores from the polymer surface to the silica surface (see also Figure 4a, Scheme 2a). The microstructure and the sintering behavior of this nascent polymer film will be discussed in due detail in a forthcoming publication.[24]

The physisorbed complex **II** activated with $B(C_6F_5)_3$ (catalyst C) produces polymer with an entirely different morphology (Figure 2). The catalyst loading can be estimated from eq 1, which arrives at about 3 Ti/nm^2. This represents slightly more than monolayer coverage. However, the catalyst/activator does not spread out on the silica wafer but precipitates to form flat, roundish islands. Upon polymerization (60 °C, 12 h, 1.6 bar C_2H_4) these islands grow to form ball-shaped, highly porous polymer beads with dimensions of up to several 10 μm. The lack of catalyst support interaction prevents the homogeneous dispersion of the catalyst on the support. The polymer beads show a high degree of porosity and the extensive formation of stress fibrils indicating in a three-dimensional growth like an expanding universe (see also Figure 4b, Scheme 2b).

The MAO-activated complex **I** (catalyst **B**) shows intermediate behavior. The catalyst/MAO mixture initially forms a thin film (roughly 50 nm as derived from SEM) on the flat silica, which is largely homogeneous but also shows some small grains and wave patterns (the later seem to be induced by small ubiquitous dust particles). These irregularities develop into much larger structures during polymerization. Some craterlike structures of several micrometers resemble the polymer beads on the physisorbed system **C** and thus represent an area of localized high activity (hotspot) most probably due to a clustering of active species (Figure 3). At the homogeneous region, however, we observe the formation of polymer films (see also Figure 4c, Scheme 2c). Obviously MAO prevents the agglomerization of the metallocene on the silica support to some extent. This increases the dispersion of the active sites on the catalyst and induces controlled one-dimensional film growth.

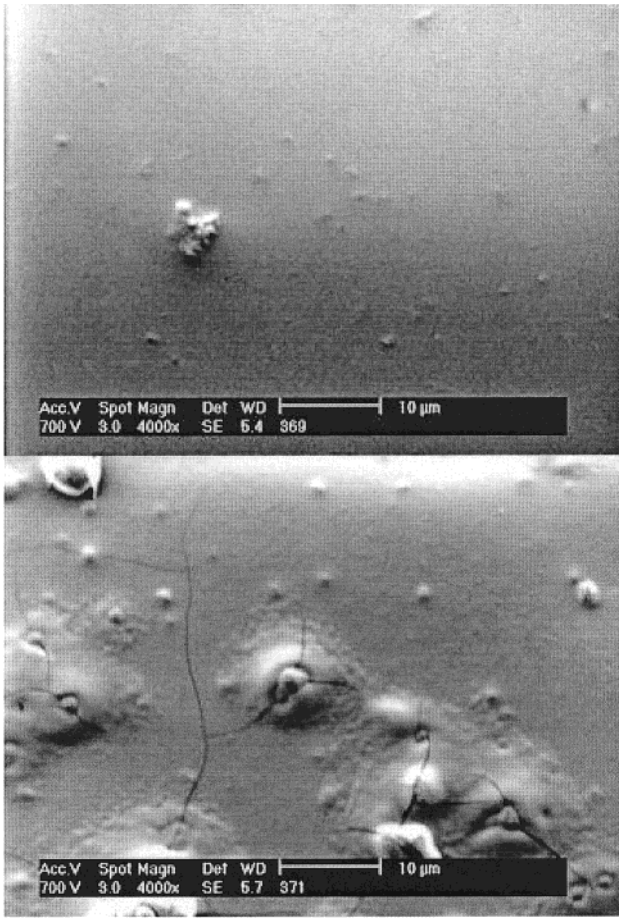

Figure 3. Surface overview of *rac*-[Me_2Si(2-Me-4-(1-Naph)-Ind)$_2$]$ZrCl_2$−MAO/SiO_2/Si(100) after spin-coating impregnation (top) and after ethylene polymerization (60 °C, 1.6 bar ethylene, 12 h, bottom).

Interestingly we find the polymer to be covered by a layer of almost 50 nm MAO residue (confirmed by EDX, not shown). Most of the MAO/catalyst mixture seems to be deactivated by trace amounts of water and oxygen in the glovebox ambient before the polymerization starts. Such a deactivation is not unexpected, even in a glovebox environment, considering the extreme activity of MAO toward water and the constant flow of fresh glovebox ambient over the catalyst surface during spin-coating. As catalyst deactivation is a very fast reaction we observe a very sharp interface between toplayer (the deactivated catalyst) and polymer after polymerization. This toplayer obviously does not prevent ethylene from reaching the active polymerization zone. We therefore propose that it has no direct influence on the polymer morphology that evolves.

At this stage it is difficult to judge whether a true anchoring of the active centers by silica bound MAO-species induces the 1-dimensional film growth or whether the catalyst MAO mixture only forms a more or less homogeneous film or a combination of both. Attempts to elucidate this question by sequential polymerization of ethylene and propylene did not reveal any sign of sequential polyethylene/polypropylene layers, which may support the homogeneous film proposition. Commercial silica/MAO supports comprise a typical Si/Al ratio of 1, which is equivalent to a MAO layer of approximately 3 nm (assuming a 300 m^2 surface area). This is about 1 order of magnitude less than on the flat model catalyst. Still, our main observation may be valid also on MAO pretreated silica. MAO facilitates the homogeneous dispersion of the catalyst on the silica surface but may do so by serving as a diluent matrix preventing catalyst clustering rather than as a true anchor to the silica surface. Figure 4 gives a comparison of the polymer morphologies that evolve on the three catalytic systems under discussion.

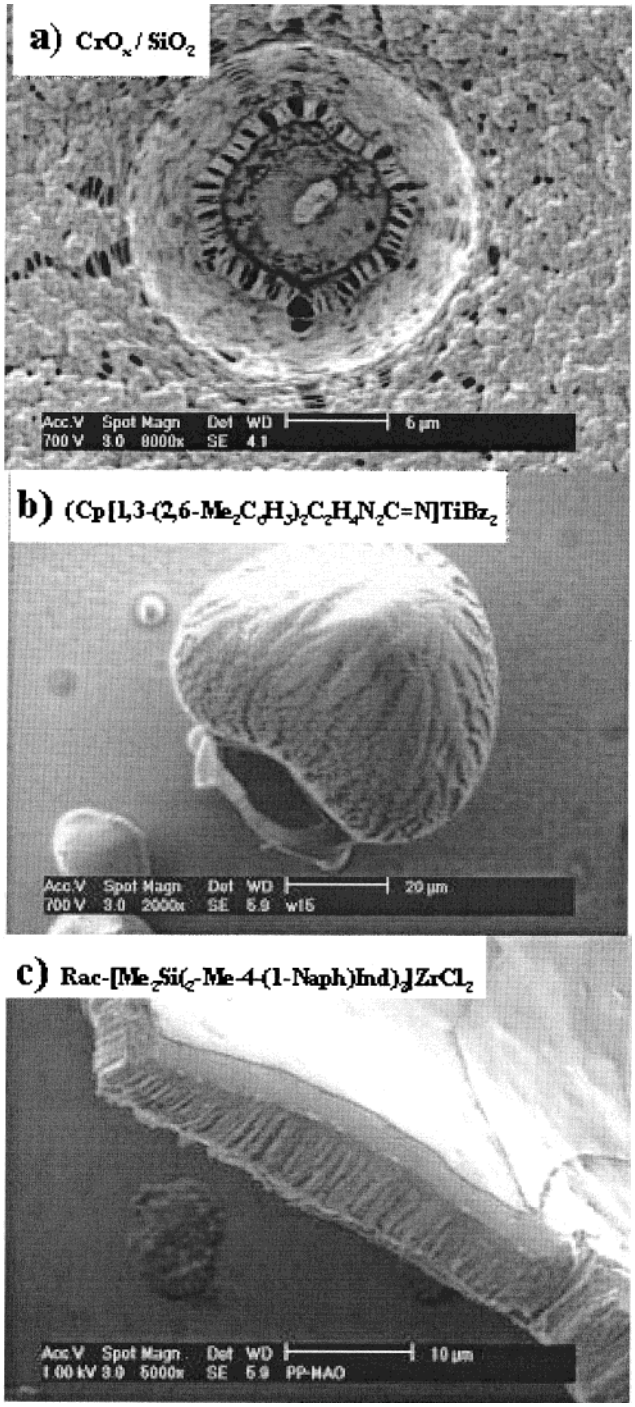

Figure 4. Comparing polymer morphology: (a) inside view of polyethylene film grown on from well-dispersed anchored polymerization centers (CrO_x/SiO_2/Si(100)), (b) highly porous polyethylene bead with extensive formation of stress fibrils as result of three-dimensional polymer growth (Cp[1,3-(2,6-$Me_2C_6H_3$)$_2C_2H_4N_2C$=N]$TiBz_2$−B(C_6F_5)$_3$/SiO_2/Si(100)), and (c) polypropylene film covered by approximately 50 nm of MAO residue *rac*-[Me_2Si(2-Me-4-(1-Naph)Ind)$_2$]$ZrCl_2$−MAO/SiO_2/Si-(100).

Because of the very small amounts of polymer that we produce on the flat model supports (no more than a few micrograms in total), our possibilities for polymer analysis are at present limited to simple Infrared and Raman microscopy. Thus, we cannot elaborate on the microstructure of the polymer chains at this stage. These issues are beyond the scope of this introduction. However, we can give an estimation of the polymerization activity and compare these activities to the real heterogeneous systems. The Phillips model systems produces about 20 μm of polyethylene at 90 °C within 12 h at 1.6 bar, which scales to about 200 g/(g_{cat}·h·bar), assuming the bulk density of melt-crystallized PE for the nascent polymer film and scaling to a 300 m^2/g silica support. A typical Phillips catalyst should produce about 100−300 g/(g_{cat}·h·bar) at 100 °C.[25] The MAO-activated catalyst **I** gives about 10 μm polypropylene after 12 h corresponding to about 100 g/(g_{cat}·h·bar). This value is very difficult to compare to literature values, as we do not know the portion of active catalyst. However, Arrowsmith et al.[26,27] have measured the activity of the Kat I/MAO/SiO_2 system. The gas-phase activities of these catalysts calculate to about 4 g/(g_{cat}·h·bar) with a catalyst loading that is about 1% of ours. The activity of Cp[1,3-(2,6-$Me_2C_6H_3$)$_2C_2H_4N_2C$=N]$TiBz_2$−B(C_6F_5)$_3$/SiO_2/Si(100) is very difficult to estimate as we observe ball-shaped polymer beads instead of a more or less smooth film. Nevertheless, we can give an order-of-magnitude estimation from the size distribution of the polymer beads. We arrive at a film thickness of 250 nm to 1 μm after 12 h, which corresponds to no more than 10 g /(g_{cat}·h·bar).

Conclusions

Following the example of the flat CrO_x/SiO_2/Si(100) (Phillips) ethylene polymerization catalyst, we have explored the possibilities to support "single site" polymerization catalysts on a flat silica surface to gain additional knowledge in the heterogenization procedure of these homogeneous catalysts especially in relationship to the polymer morphology that develops during polymerization. The catalyst dispersion and the development of the observed polymer morphologies are sketched in Scheme 2. Our initial results already demonstrate the potential of this approach.

- Even though the total amount of catalyst during a polymerization is only a few nanomoles it remains active for ethylene polymerization.
- The morphology of the growing polymer films in the micrometer range is readably visualized by SEM and reflects the dispersion of the active phase and the strength of the catalyst support interaction.
- The defined geometry of the flat support facilitates the interpretation of the observed polymer morphologies
- Strong chemical interaction with the support, such as direct chemical bonds give rise to homogeneous polymer films with a single growth direction in the direction of the surface normal of the flat support.
- Homogeneous dispersion of active sites inside a MAO matrix, which itself forms a film on the silica film, is also sufficient to let the polymer grow as a film; however, inhomogeneities in the MAO matrix results in hot spots
- Lack of catalyst support interaction results in clustering of the active phase during drying. These clusters grow in a three-dimensional fashion resulting in a highly porous polymer with extensive formation of stress fibrils.
- Due to the very small amounts of polymer that we produce (no more than a few micrograms in total), we cannot elaborate on the microstructure of the polymer chains

Aiming at a deeper understanding and control of the nascent polymer morphology, we intend to explore the possibilities for flat olefin polymerization catalysts further. The logical next steps are more sophisticated heterogenization procedures to create anchored catalyst precursor or cocatalyst.[28] This should lead to better defined polymerization catalysts, including the detailed surface characterization at every stage of the synthesis and finally the study of the very early stages of polymer film growth.

Scheme 2. Schematic Representation of Catalyst Dispersion (Left) and Polymer Growth (Right)[a]

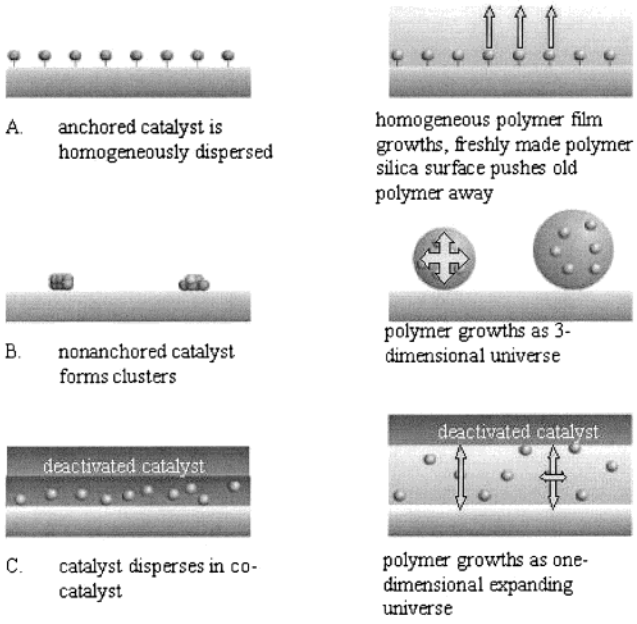

[a] Key: (A) Active sites are anchored to the silica support (Phillips system); the new polymer is formed on the silica surface and pushes previously made polymer away. (B) Active species aggregate to islands (Cp[1,3-(2,6-$Me_2C_6H_3$)$_2C_2H_4N_2C$=N]-$TiBz_2$-B(C_6F_5)$_3$). Upon polymerization, these islands grow in three dimensions with the active sites expanding in the growing polymer bead. (C) Active species are dispersed in a matrix of cocatalyst (*rac*-[Me_2Si(2-Me-4-(1-Naph)Ind)$_2$]$ZrCl_2$-MAO). Polymer is formed within that matrix and polymerization centers are mobile; however, due to the homogeneous dispersion of active sites the film can only grow in the direction of the surface normal.

References and Notes

(1) Sinn, H.; Kaminski, W. *Adv. Organomet. Chem.* **1980**, *18*, 99−149.
(2) Kaminski, W. *Makromol. Chem. Phys.* **1996**, *197*, 3907−3945.
(3) Coates, G. W. *Dalton Trans.* **2002**, 4674−475.
(4) Brintzinger, H. H.; Fischer, D.; Mühlhaupt, R.; Rieger, B.; Waymouth, R. *Angew. Chem.* **1995**, *107*, 1255−1270.
(5) Resconi, L.; Cavallo, L.; Fait, A.; Piemontesi, F. *Chem. Rev.* **2000**, *100*, 1253−1345.
(6) Carnahan, E. M.; Grant, B. J *CATTECH* **2000**, *4* (1), 74−88.
(7) Hlatky, G. G. *Chem. Rev.* **2000**, *100*, 1347−1376.
(8) Karol, F. J.: *Macromol. Symp.* **1995**, *89*, 563−575.
(9) Hogan, J. P.; Norwood, D. D.; Ayres, C. A. *J. Appl. Polym. Sci., Appl. Polym. Symp.* **1981**, *36*, 49−60.
(10) Kaminsky, W.; Winkelbach, H. *Top. Catal.* **1999**, *7*, 61−67.
(11) Duchateau, R.; van Santen, R. A.; Yap, G. P. A. *Organometallics* **2000**, *19*, 809−816.

(12) Duchateau, R.; Abbenhuis, H. C. L.; van Santen, R. A.; Thiele, S. K. H.; van Tol, M. F. H. *Organometallics* **1998**, *17*, 5222−5224.
(13) Gunter, P. L. J.; Niemantsverdriet, J. W.; Ribeiro, F. H.; Somorjai, G. A. *Catal. Rev.—Sci. Eng.* **1997**, *39*, 77−168.
(14) de Jong, A. M.; de Beer, V. H. J.; van Veen, J. A. R.; Niemantsverdriet, J. W. *J. Phys. Chem.* **1996**, *100*, 17722−177724.
(15) Thüne, P. C.; Verhagen, C. P.; van den Boer, M. J.; Niemantsverdriet, J. W. *J. Phys. Chem. B* **1997**, *101*, 8559−8563.
(16) Thüne, P. C.; Loos, J.; Lemstra, P. J.; Niemantsverdriet, J. W. *Top. Catal.* **2000**, *13*, 67−74.
(17) Thüne, P. C.; Linke, R.; van Gennip, W. J. H.; de Jong, A. M.; Niemantsverdriet, J. W. *J. Phys. Chem. B* **2001**, *105*, 3073−3078.
(18) van Hardeveld, R. M.; Gunter, P. L. J.; van IJzendoorn, L. J.; Wieldraaijer, W.; Kuipers, E. W.; Niemantsverdriet J. W. *Appl. Surf. Sci.* **1995**, *84*, 339−346.
(19) Spalek, W.; Küber, F.; Winter, A.; Rohrmann, J.; Bachmann, B.; Antberg, M.; Dolle, V.; Paulus, E. F. *Organometallics* **1994**, *13*, 954−963.
(20) Kretschmer W. P. WO 02/070569 (Dutch Polymer Institute) 2002.
(21) Kretschmer, W. P.; Dijkhuis, C.; Meetsma, A.; Hessen, B.; Teuben, J. H. *Chem. Commun.* **2002**, 608−609.
(22) Massey, A. Y.; Park, A. J. *J. Organomet. Chem.* **1964**, *2*, 245−250.
(23) Thüne, P. C.; Loos, J.; Lemstra, P. J.; Niemantsverdriet, J. W. *J. Catal.* **1999**, *183*, 1−5.
(24) Loos, J.; Thüne, P. C.; Niemantsverdriet, J. W.; Lemstra, P. J. Manuscript in preparation.
(25) Choi, K.-T.; Ray, W. H. J. *Macromol. Sci. Macromol. Chem. Phys.* **1985**, *25*, 57−97.
(26) Arrowsmith, D.; Kaminsky, W.; Laban, A.; Weingarten, U. *Macromol. Chem. Phys.* **2001**, *202*, 2161−2167.
(27) Kaminsky, W.; Arrowsmith, D.; Laban, A.; Lemstra, P. J.; Loos, J.; Weingarten, U. *Chem. Eng. Technol.* **2001**, *24*, 1124−1128.
(28) E.g.: Walzer, J. F. WO 9604319 (Exxon Chemical Patents Inc.) 1996.

MA021007Z